Original Article

K^{trans} Calculation Using Reference Method Corrected Native T_{10} for Breast Cancer Diagnosis

Pradeep Singh Negi[1,2], Shashi Bhushan Mehta[1,2], Amarnath Jena[1,2], Prerana Rana[1]

[1]PET Suite (Indraprastha Apollo Hospitals and House of Diagnostics), Department of Molecular Imaging and Nuclear Medicine, Indraprastha Apollo Hospitals, New Delhi, [2]Department of Physics, Vivekananda Global University, Jaipur, Rajasthan, India

Abstract

Purpose: The objective of the study is to use multiple tube phantoms to generate correction factor at different spatial locations for each breast coil cuff to correct the native T_{10} value in the corresponding spatial location of the breast lesion. The corrected T_{10} value was used to compute K^{trans} and analyze its diagnostic accuracy in the classification of target condition, i.e., breast tumors into malignant and benign. **Materials and Methods:** Both *in vitro* phantom study (external reference) and patient's studies were acquired on simultaneous positron emission tomography/magnetic resonance imaging (PET/MRI) Biograph molecular magnetic resonance (mMR) system using 4 channel mMR breast coil. The spatial correction factors derived using multiple tube phantom were used for a retrospective analysis of dynamic contrast-enhanced (DCE) MRI data of 39 patients with a mean age of 50 years (31–77 years) having 51 enhancing breast lesions. **Results:** Corrected and non-corrected receiver operating characteristic (ROC) curve analysis revealed a mean K^{trans} value of 0.64 min^{-1} and 0.60 min^{-1}, respectively. The sensitivity, specificity, positive predictive value (PPV), negative predictive value (NPV), and overall accuracy for non-corrected data were 86.21%, 81.82%, 86.20%, 81.81%, and 84.31%, respectively, and for corrected data were 93.10%, 86.36%, 90%, 90.47%, and 90.20% respectively. The area under curve (AUC) of corrected data was improved to 0.959 (95% confidence interval [CI] 0.862–0.994) from 0.824 (95% CI 0.694–0.918) of non-corrected data, and for NPV, it was improved to 90.47% from 81.81%, respectively. **Conclusion:** T_{10} values were normalized using multiple tube phantom which was used for computation of K^{trans}. We found significant improvement in the diagnostic accuracy of corrected K^{trans} values that results in better characterization of breast lesions.

Keywords: Dynamic contrast-enhanced magnetic resonance imaging, K^{trans}, molecular magnetic resonance breast coil, T_{10}

Received on: 24-09-2022 **Review completed on: 12-12-2022** **Accepted on: 21-12-2022** **Published on: 18-04-2023**

Introduction

Cancer is a leading cause of death in women before the age of 70 years and breast cancer is the most commonly diagnosed cancer in women among all other cancers.[1] Dynamic contrast-enhanced magnetic resonance imaging (DCE-MRI) of the breast is the modality of choice to characterize tumor into malignant and benign. The pattern of the contrast enhancement in the tumor tissue over a period of time, i.e., time activity curve of tumor in routinely done high spatial resolution DEC-MRI, can characterize the tumor tissue based on three types of curves, i.e., (1) wash in and wash out (curve Type 3) denoting malignant characteristic, (2) initial rise and plateau (curve Type 2) denoting indeterminate: either benign or malignant characteristic, and (3) persistent rise (curve Type 1) denoting benign characteristic. However, the classification of a lesion on DCE-MRI as benign or malignant still remains a challenge.[2-8]

Access this article online

Quick Response Code:

Website: www.jmp.org.in

DOI: 10.4103/jmp.jmp_90_22

Pharmacokinetic (PK) parameters, i.e., transfer constant (K^{trans}), extracellular volume (v_e), and flux rate constant (k_{ep}) rely on the quantification of vascular events through compartmental modeling. It is a highly potential method to classify the tumor into benign or malignant groups. A sharp rise in the enhancement curve is reported in the malignant tissue as compared to benign and normal tissues of the breast because of the neoangiogenesis in the malignant tissues.[8-11] High and low K^{trans} values of the tumor denote the malignant and benign tissue, respectively. K^{trans}, which is a quantitative parameter, is

Address for correspondence: Dr. Pradeep Singh Negi, Department of Molecular Imaging and Nuclear Medicine, Pet Suite, Indraprastha Apollo Hospitals, SaritaVihar, Delhi–Mathura Road, New Delhi - 110 076, India.
E-mail: pradeepnegi1979@gmail.com

How to cite this article: Negi PS, Mehta SB, Jena A, Rana P. K^{trans} calculation using reference method corrected native T_{10} for breast cancer diagnosis. J Med Phys 2023;48:19-25.

known to be influenced by a host of interlinked factors. These factors mostly include a large field of view (FOV) required for bilateral breast imaging, off-center positioning of the patient's torso inside the transmitting whole-body radiofrequency (RF) birdcage coil thus resulting in unequal loading effects and RF nonlinearity in the transmitter/receiver system or coils are factors that influence B_1 homogeneity causing flip angle error in the magnetic resonance (MR) pulse sequence.[12] These factors can propagate error in the computation of native T_1, which is a key factor in the computation of K^{trans}. Many researchers had focused to correct the flip angle by improving B_1 homogeneity across the breast coil cuffs and that in turn corrected the T_{10} at each spatial location to improve K^{trans} computation.[13-19] Other factors affecting K^{trans} computation are arterial input function (AIF) and time-intensity curve of the lesion. AIF which is influenced by high temporal resolution data sampling is mostly addressed through fast MRI sequences and high-field magnet system. Suitable mathematical modeling has been used to achieve accurate curve fit of the time-intensity curve. To reduce the acquisition time (TA) in the calculation of K^{trans}value while still maintaining the adequate diagnostic accuracy has been a matter of research.[20-22] These observations underscored the fact that factors influencing the estimation of K^{trans} needs to be adequately addressed so that it can be used as a reliable parameter in the clinical setting. Many approaches such as variable flip angle (VFA): multiple flip angles (MFA), dual flip angle (DFA), and driven equilibrium single pulse observation of T_1 with high-speed incorporation of RF field in homogeneities (DESPOT1-HIFI) etc have been used to improve T_{10} by correcting the B_1 inhomogeneity.[20-24] The most common method used to derive T_{10} is using VFA; in this method, multiple data points were sampled to correct the flip angle errors which improves the computational accuracy of T_{10}.[16-19,22-27] It has also been reported that DFA with 2° and 15° flip angles; takes lesser TA than MFA, gives results nearest to the MFA technique for the assessment of PK parameters in the head-and-neck malignancies.[22] In the last few years, Jena *et al*. tried to directly normalize T_{10} values in bilateral breast tissue instead of B_1 correction of breast coil cuffs.[20,21] In that method, a single tube phantom prefilled with a material of known T_1 value was used as an external standard for native T_1 correction and the corrected T_{10} was used for the computation of K^{trans} values. That method was found useful in improving the diagnostic accuracy of K^{trans} in clinical cases. Later on, Negi *et al*.[28] adopted an *in vitro* reference method to normalize T_1 distribution using an in-house designed multiple tube phantom placed within the breast coil cuffs and T_1 was calculated using DFA protocol. The T_1 values were normalized in the molecular magnetic resonance (mMR) breast coil-cuff by applying correction factors derived for each spatial location and observed that before the application of correction factors, T_1 distribution was inhomogeneous in different parts of each breast coil cuff as well as between the left and right coil cuff. The homogeneity improved in mMR breast coil after correction.[28]

In contrast to earlier literatures, where researchers attempted to homogenize the B_{10} distribution[16-19] that was ultimately used to correct the T_{10} value, our current study aimed to use the index test, i.e., multiple tube phantom to generate correction factor at different spatial locations for each breast coil cuff to correct the native T_1 value in the corresponding spatial location of the breast lesion. The corrected T_{10} value was then used to compute the K^{trans} and analyze its diagnostic accuracy in the classification of target condition, i.e., breast tumors into malignant and benign.

Materials and Methods

Both *in vitro* phantom study and retrospective patient's studies were acquired on simultaneous positron emission tomography (PET/MRI) Biograph mMR system 3.0 T (Siemens, Erlangen, Germany) using 4 channel mMR breast coil. The acquisition of phantom image was done using DFA method to derive correction factor for T_1 value at each spatial location.[28] The correction factor so obtained was then applied to Native T_{10} values of breast lesions of 39 patients that was spatially synchronized with the lesion. The patients were selected consecutively from the database between 2018 and 2021 with a mean age of 50 years (31–77 years) having a total 51 lesions who had undergone breast PET/MRI study as part of their diagnostic/staging workup with proven cancer on histopathology before or done subsequently after their PET/MRI scan. The demography of the study cohort is given in Table 1. The study protocol was approved by the ethics committee of the institute and waiver of consent was allowed owing to the retrospective nature of study related to patients.

Phantom creation and study

In Multiple tube phantoms, each phantom contains 19 tube that were filled with the contrast solution i.e., water and Gd-DTPA ([diethylenetriamine pentaacetic acid gadodiamide (Omniscan)]; 0.1 mMol) which was mixed in the ratio of 10:1. The phantom was designed in such a way

Table 1: Demography of study cohort

Cohort Characteristics	*n*		
Study cohort	39		
Mean age (range) (years)	50 (31-77)		
	Right breast	**Left breast**	**Total number**
Enhancing lesions	25	26	51
Benign	9	13	22
Malignant	16	13	29
Characterisation of lesions based on HPE			
Benign	***n***	**Malignant**	***n***
FA	19	IDC	27
FCD	3	DCIS	2

HPE: Histopathology, FA: Fibroadenoma, FCD: Fibrocartilaginous dysplasia, IDC: Invasive ductal carcinoma, DCIS: Ductal carcinoma *in situ*

that it would fully occupy the cuff space when placed inside the breast coil [Figure 1].

Phantoms were positioned one in each cuff, corresponding to the isocenter of the magnet using light localizer. After localizer images obtained, 2° flip angle proton density and 15° flip angle non-fat suppressed T1-weighted images volumetric interpolated body examination (VIBE) with time to echo (TE) 1.8 ms, repetition time (TR) 5.2 ms, FOV 360 mm, slices 24, TA 12.3 s, resolution 256 × 256 and voxel size 3.9 mm × 1.4 mm × 4.0 mm[21,24] were acquired for computation of T_1 value at each spatial location (total of 684 data locations for each coil cuff: 19 tubes × 36 slices) [T_1 values were calculated using Equation 1 of Supplementary Materials].

Patient studies and synchronization with phantom study

All patients were imaged in the prone position with each breast placed in the breast coil cuff at the isocenter of the magnet. Patients had undergone high temporal resolution, i.e., 4.1 s postcontrast 15° VIBE (TE 1.8 ms, TR 5.2 ms, FOV 360 mm, slices 24, TA 4.1s, resolution 256 × 256, and voxel size 3.9 mm × 1.4 mm × 4.0 mm) with a total TA of ~60 s; this imaging protocol was sandwiched in a routine high spatial resolution DCE MRI.[20]

Precontrast 15° images subtracted from the last postcontrast series of dynamic data was used for localizing enhancing lesion in the breast parenchyma. MRI protocols were performed in a fix table position with the same matrix size (256 × 256) for both phantom study and patient's study for inter-study (phantom study and patient study) spatial correlation. Since both patient and phantom study were done using the same breast coil, the correction factor achieved from the phantom for each x, y coordinate of the breast coil space remain same for the corresponding (x, y coordinate) of the breast image done using the same breast coil. When the lesion is located between multiple tubes, then we had taken averaged correction factor value of all surrounding tubes for that spatial location. The same method was applied for large-size lesion covering more than one tube; in this scenario, the average correction value of all involved tubes was taken. The correction factors derived by the phantom study, nearest or overlapped to the breast lesion were applied to the lesions in all 39 patients to correct the T_{10} values and used for computing K^{trans} values. The K^{trans} values in breast lesions before and after applying the correction factor were compared to verify the diagnostic accuracy of this method [Details of T_{10} correction and K^{trans} computation are described in the Supplementary Materials and Supplementary Figures 1-4]. Region of interest (ROI) drawn on visible breast lesion on the 15° flip angle subtracted image, was copied and pasted on the corresponding 2° flip angle image and all postcontrast 15° dynamic series for native T_1 and K^{trans} calculation. Both patient and phantom study were spatially synchronized using Syngovia software (version VB 10B, M/s, Siemens Healthineers, Germany), [Figure 2].

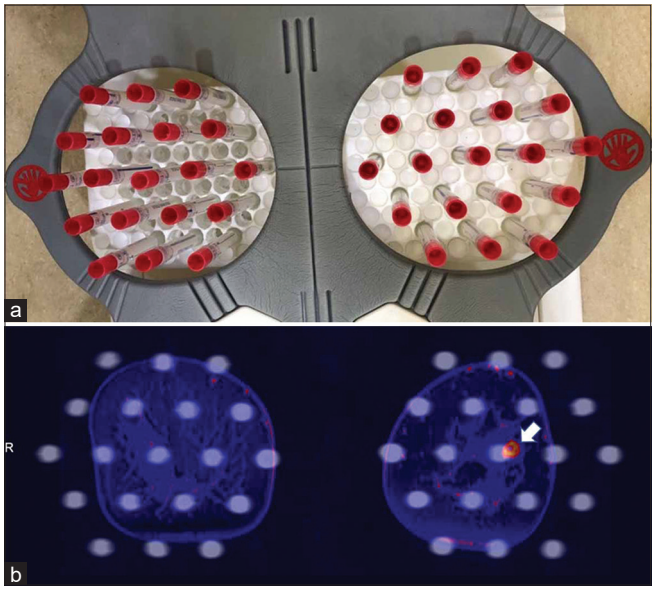

Figure 1: (a) Showing multiple tube phantom (19 tubes) filling the space of both cuffs of breast coil. (b) Both patient and phantom study spatially synchronized using Syngovia software: The correction factor of the nearest tube to the tumor highlighted by arrow, was applied to correct the T_{10} of tumor

Statistical analysis

The two-tailed paired *t*-test was performed between corrected and non-corrected K^{trans}, and corrected and non-corrected T_{10} value which was divided into malignant and benign groups. The corrected and non-corrected K^{trans} values were correlated with the clinical reference standard, i.e., histopathological findings. Using logistic regression analysis for both corrected and non-corrected K^{trans} data, the true positive, true negative, false positive, false negative, and accuracy were calculated. Receiver operating characteristic (ROC) curve analysis on this data was done to calculate area under curve (AUC), sensitivity, and specificity. The power of the study was calculated to be 82%. The statistical analysis was performed using MedCalc

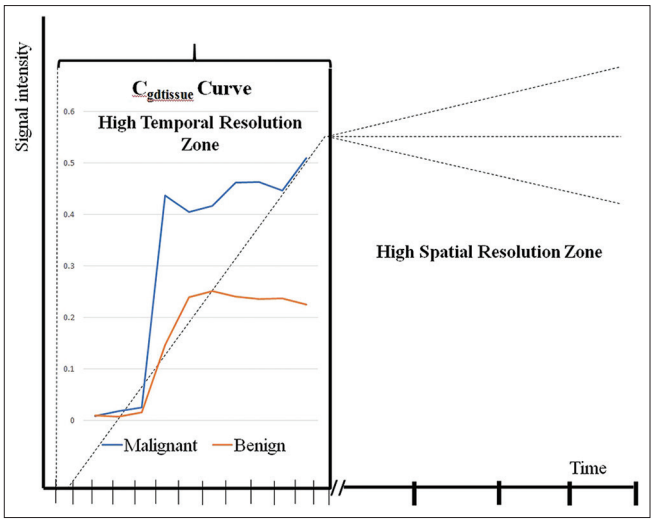

Figure 2: The schematic diagram of sandwiched protocol showing time intensity graph and $C_{gdtissue}$ curve (for K^{trans} calculation) of malignant and benign breast lesion

statistical software package (version 19.8-64 bit (MedCalc Software Ltd, Ostend, Belgium); Windows Vista/7/8/10). A P value < 0.05 was considered to be statistically significant. The tumor T_{10} difference between the left and right breast was calculated by subtracting the T_{10} values of the right and left breast divided by greater value of T_{10} between the two, in the end, the result was multiplied by 100.

Results

Phantom study

The difference in T_1 values observed across ROIs between right and left side of breast coil was significant ($P < 0.001$). After correction, no significant difference was noted suggesting convergence of mean T_1 value and regression of standard deviation ($P = 0.091$) across spatial locations in the coils. The mean T_1 value before the correction was 6.08 ± 1.02 ms and 5.38 ± 1.06 ms in right and left breast coil, respectively, which after correction was changed to 6.12 ± 0.26 ms and 6.03 ± 0.28 ms.

Patient study

The estimated T_{10} values of 51 (22 benign and 29 malignant) enhancing breast lesions without phantom correction were 1469 ± 310 ms in the left breast and 1832 ± 527 ms in the right breast which was found to be statistically significant at a $P = 0.004$. However, while the estimated T_{10} values of tumor with phantom correction were 1590 ± 476 ms in the left breast and 1737 ± 611 ms in the right breast which was found to be statistically insignificant, i.e., $P = 0.34$. The difference between T_{10} value of the right and left breast was statistically insignificant after correction [a detailed distribution of T_{10} values in breast coil is given in Supplementary Table 1]. The tumor T_{10} difference between the left and right breasts was 19.8%, which was reduced to 8.4% after correction. The average size of the malignant lesions was 3.37 cm (range: 0.8–8.4 cm) and of benign lesions was 2.41 cm (range: 0.7–11.7 cm). The results for the mean of corrected and non-corrected K^{trans} for benign and malignant lesions are summarized in Table 2. The mean of non-corrected K^{trans} value for malignant lesions was 0.81 ± 0.83 min^{-1} and corrected K^{trans} value was 0.92 ± 0.75 min^{-1} ($P = 0.01$). The mean of non-corrected K^{trans} value for benign lesions was 0.30 ± 0.24 min^{-1} and for corrected K^{trans} value was 0.27 ± 0.18 min^{-1} [$P = 0.008$, Figure 3].

The mean K^{trans} of total lesions (benign + malignant) before correction was 0.60 min^{-1} and after correction was 0.64 min^{-1}. Before correction 4 patients were false positive and 4 patients were false-negative with a 0.38 min^{-1} cut-off value for K^{trans} and after correction, it was 3 false positive and 2 false negative with 0.50 min^{-1} cutoff.

Corrected and non-corrected ROC curve analysis revealed a mean K^{trans} value of 0.64 min^{-1} and 0.60 min^{-1}, respectively. The sensitivity, specificity, positive predictive value (PPV), negative predictive value (NPV) and overall accuracy for non-corrected data were 86.2%, 81.8%, 86.2%, 81.8%, and 84.3%, respectively, and for corrected data, the values were 93.1%, 86.3%, 90%, 90.4%, and 90.2%, respectively. The AUC for non-corrected data was 0.82 (95% confidence interval [CI] 0.69–0.91) and for corrected data were 0.95 (95% CI 0.86–0.99) [Figure 4]. The AUC was improved from 0.82 to 0.95 and also NPV was improved from 81.8%–90.4%.

Discussion and Conclusion

Reliable estimation of T_{10} of tissue under investigation is a prerequisite for accurate measurement of PK parameters. This assumes importance because of increasing application of PK parameters to assess the neoangiogenesis property of cancer, in particular breast cancer diagnosis, to use it as a response evaluation tool in future and to assess the efficacy of newer coming drugs.[13,14,16-18]

In this study, we tried to improve the accuracy of PK parameters by directly normalizing T_{10} at each spatial location of breast coil cuffs by applying correction factor derived from the phantom study. Our approach was different from other workers who had worked on homogenizing the B_{10} distribution[16-19] that ultimately helped to achieve more accurate T_{10} value.

This technique was using multiple correction factors at different spatial locations for each breast coil cuff to correct

Table 2: Effect of multiple tube phantom on T_{10} and K^{trans} in breast lesions

Parameters	Right		Left		Both sides	
	Non-corrected	Corrected	Non-corrected	Corrected	Non-corrected	Corrected
Malignant						
K^{trans} (mean±SD)	0.98±1.06	1.10±0.96	0.60±0.22	0.70±0.18	0.81±0.83	0.92±0.75
					P=0.01	
Range	0.15-4.11	0.57-3.37	0.26-1.02	0.41-1.10	0.15-4.11	0.41-3.37
T_{10} (mean±SD)	1828±292	1591±237	1392±177	1370±291		
Benign						
K^{trans} (mean±SD)	0.30±0.24	0.27±0.18	0.33±0.21	0.27±0.15	0.31±0.22	0.27±0.16
					P=0.008	
Range	0.08-0.94	0.08-0.71	0.09-0.75	0.08-0.58	0.09-0.94	0.05-0.71
T_{10}	1838±768	1996±889	1546±376	1809±505		

Values are mean±standard deviation. SD: Standard deviation

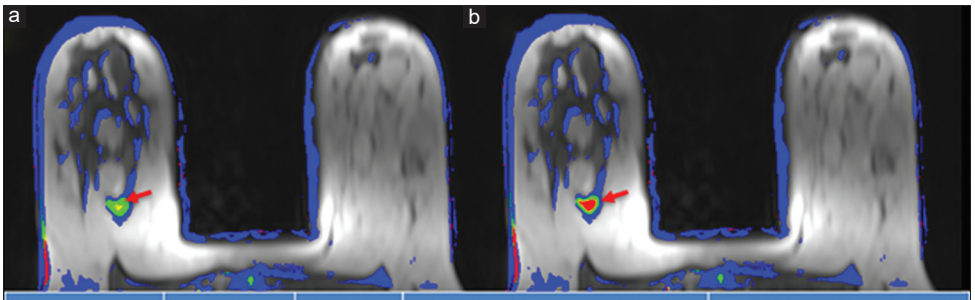

	T_{10}	K^{trans}	Tumor Characterisation based on K^{trans}	Final Diagnosis based on HPE
non-corrected	1309.66	0.30	Benign	Invasive ductal carcinoma
Corrected	1121.28	0.57	Malignant	

Figure 3: The effect of T_{10} correction on characterization of lesion based on its K^{trans} value. Non-corrected image of lesion. (a) showing benign nature i.e., yellow and green color and after correction the image. (b) of the same lesion shows malignant nature i.e., red in color. (As pointed out by arrow)

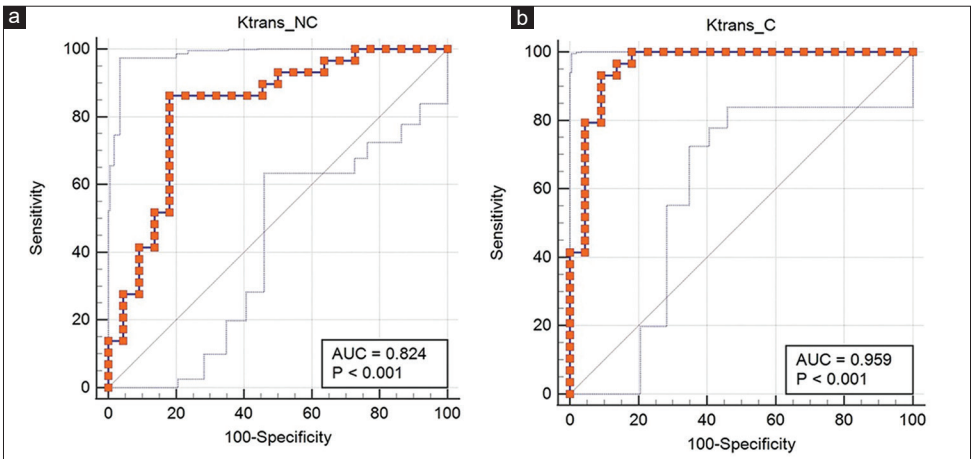

	Sensitivity	Specificity	Accuracy	PPV	NPV	AUC	95% CI	standard error	True positive	True Negative	False Positive	False Negative
Ktrans_C	93.1	86.36	90.2	90	90.47	0.959	0.862 to 0.994	0.0288	27	19	3	2
Ktrans_NC	86.21	81.82	84.31	86.2	81.81	0.824	0.694 to 0.918	0.062	25	18	4	4

Figure 4: ROC curve and results of statistical analysis of non-corrected. (a) and corrected (b) K^{trans}. ROC: Receiver operating characteristic

the native T_1 value in the corresponding spatial location of the breast lesion compared to the study of Jena *et al*. which was using a single correction factor for both coil cuffs that were not spatially synchronized with the breast lesion thus making our method technically different than single tube phantom technique.[20-21] The current method of multiple tubes had the advantage of having correction factors at multiple spatial locations in the cuff space that can be applied directly to the nearby or overlapping tumor which makes the technique more robust.

Unlike other workers who had used MFA,[16-19,23,24,26,27,29,30] we were using DFA (2° and 15°) to calculate T_{10}, that has been reported to give results nearest to MFA for PK parameters estimation[22] with lesser scan time. This lesser scan time helped in the formulation of sandwiched imaging protocol in this study to adopt ~1.0 min TA slot for high temporal resolution sequences (at 4.1 s with 14 data points) in a routine DCE MRI study. The temporal resolution and TA are important parameters in the computation of K^{trans}. Each is associated with its own limitations and there is a trade-off between imaging volume with temporal resolution that ultimately effects the signal-to-noise ratio of the image; and also, between clinically acceptable time-conserving imaging protocol with diagnostic accuracy. Attempts had been made by Veltman *et al*. in 2008 to design time efficient imaging protocol by including a high temporal resolution protocol within a routine high spatial resolution DCE-MRI of the breast for patient comfort.[25] Jena *et al*. had computed K^{trans}at various time of acquisition, i.e., between 30 s and 90 s and demonstrated comparable diagnostic accuracy at 60 s to 90 s data with AUC of 0.98 for K^{trans} in differentiating benign from malignant breast lesions.[20] In the current study with temporal resolution and TA of 4.1 s and ~60 s

respectively, we found AUC for K^{trans} to be 0.95 which was an improvement over the study by Veltman *et al*. who had AUC of 0.82[25] using 4.1 s temporal resolution and 90 s TA. Tsai *et al*.[16] also used shorter temporal resolution and TA of 4.49 s and 90 s, respectively, in their study though they have only studied malignant lesions.

In our study, we found that mean T_{10} value of malignant lesions was overestimated by 1.60% in the left breast and overestimated by 12.9% in the right breast. The mean T_{10} value of benign lesions was underestimated by 17% in the left breast and underestimated by 8.59% in the right breast. This was in line with the study of Tsai *et al*.[16] in which before B_1 correction T_{10} values were overestimated by 50% in the left breast and had 7% underestimation in the right breast This further substantiates our findings of the presence of T_{10} inhomogeneity across breast coils.

The primary objective of our study was to estimate K^{trans} value which was derived by directly correcting the T_{10} value and to check the diagnostic accuracy of corrected K^{trans}. There was a significant change in the mean K^{trans} value of both benign and malignant lesions after correction, i.e., $P = 0.008$ and 0.01. The mean K^{trans} value was underestimated by 16.6% in the left breast and by 12.2% in the right breast in malignant lesions. In case of benign lesions, mean K^{trans} value was overestimated by 18.2% in the left breast and overestimated by 10% in the right breast. Whereas in a study by Bedair *et al*.[17] mean K^{trans} of lesions in the right breast was decreased by 41%, and increased by 46% in the left breast after correction. Tsai *et al*.[16] used B_1 corrected and non-corrected T_{10} for the computation of PK parameters in 1.5T MRI system and found that because of T_{10} variation, i.e., in the non-B_1 corrected data, the K^{trans} value was getting 41% underestimated in left breast and 10% overestimated in the right breast.

In the studies of Bedair *et al*.[17] and Tsai *et al*.,[16] only malignant cases were enrolled and unlike them, we had enrolled patients with enhancing breast lesion and classified them into malignant and benign types on the basis of K^{trans} values. These findings were later correlated with clinical reference standard to assess the diagnostic accuracy of K^{trans}. In fact, this is the first research article in which attempt has been made to find out the diagnostic accuracy of K^{trans} in classifying breast tumors by using multiple tube phantom for spatially correcting breast coil for native T_1.

Our overall accuracy, sensitivity, NPV, PPV, AUC, and 95% CI values were improved after correction, i.e., from 84.3%, 86.2%, 81.8%, 86.2%, 0.82%, and 0.69%–0.91%, respectively, to 90.2%, 93.1%, 90.4%, 90%, 0.95%, and 0.86%–0.99%, respectively, which was in line with our assumption. Thus, it proved that phantom-generated correction factors can be synchronized with *in vivo* spatially located breast lesions.

However, we had some limitations in our study. First, the work has been done manually, and software computation will help to improve the speed and will reduce the manual errors. Second, the study had a small cohort and needs to be verified with a large sample size. Third, tissue equivalent material having T_1 value matching with the glandular tissue could be used to improve the results in a future study. Fourth, this technique is still in its infancy phase and therefore lacks in some aspects one of which is the patient effect on the homogeneity of B_1 field which thus ultimately effect Native T_1 distribution. We have planned to include this aspect in the next phase of this study. Finally, a comparative evaluation of B_1 corrected T_1 and directly corrected T_1 would have given us an insight into the relative diagnostic accuracy of computed K^{trans} between these two techniques. In conclusion, we had normalized T_{10} values using the multiple tube phantom technique, which was used for the computation of K^{trans}. We had found improvement in the diagnostic accuracy by using corrected K^{trans} values that results in a better characterization of breast lesions.

Ethical approval

All procedures performed in studies involving human participants were in accordance with the ethical standards of the institutional research committee and with the 1964 Helsinki declaration and its later amendments or comparable ethical standards.

Financial support and sponsorship

Nil.

Conflicts of interest

There are no conflicts of interest.

References

1. World Health Organizations Global Cancer Observatory; 2020. Available from: https://gco.iarc.fr/today/data/factsheets/cancers/39-All-cancers-fact-sheet.pdf. [Last accessed on 2020 Dec 23].
2. Gilles R, Guinebretière JM, Lucidarme O, Cluzel P, Janaud G, Finet JF, *et al.* Nonpalpable breast tumors: Diagnosis with contrast-enhanced subtraction dynamic MR imaging. Radiology 1994;191:625-31.
3. Hulka CA, Smith BL, Sgroi DC, Tan L, Edmister WB, Semple JP, *et al.* Benign and malignant breast lesions: Differentiation with echo-planar MR imaging. Radiology 1995;197:33-8.
4. Kelcz F, Santyr GE, Cron GO, Mongin SJ. Application of a quantitative model to differentiate benign from malignant breast lesions detected by dynamic, gadolinium-enhanced MRI. J Magn Reson Imaging 1996;6:743-52.
5. Kuhl CK, Mielcareck P, Klaschik S, Leutner C, Wardelmann E, Gieseke J, *et al.* Dynamic breast MR imaging: Are signal intensity time course data useful for differential diagnosis of enhancing lesions? Radiology 1999;211:101-10.
6. Nunes LW, Schnall MD, Orel SG, Hochman MG, Langlotz CP, Reynolds CA, *et al.* Breast MR imaging: Interpretation model. Radiology 1997;202:833-41.
7. Perman WH, Heiberg EM, Grunz J, Herrmann VM, Janney CG. A fast 3D-imaging technique for performing dynamic Gd-enhanced MRI of breast lesions. Magn Reson Imaging 1994;12:545-51.
8. Fischer U, Kopka L, Brinck U, Korabiowska M, Schauer A, Grabbe E. Prognostic value of contrast-enhanced MR mammography in patients with breast cancer. Eur Radiol 1997;7:1002-5.
9. Abe H, Mori N, Tsuchiya K, Schacht DV, Pineda FD, Jiang Y, *et al.* Kinetic analysis of benign and malignant breast lesions with ultrafast dynamic contrast-enhanced MRI: Comparison with standard kinetic assessment. AJR Am J Roentgenol 2016;207:1159-66.
10. Agrawal G, Su MY, Nalcioglu O, Feig SA, Chen JH. Significance of breast lesion descriptors in the ACR BI-RADS MRI lexicon. Cancer

2009;115:1363-80.
11. Ma ZS, Wang DW, Sun XB, Shi H, Pang T, Dong GQ, *et al.* Quantitative analysis of 3-Tesla magnetic resonance imaging in the differential diagnosis of breast lesions. Exp Ther Med 2015;9:913-8.
12. Rahbar H, Partridge SC, DeMartini WB, Thursten B, Lehman CD. Clinical and technical considerations for high quality breast MRI at 3 Tesla. J Magn Reson Imaging 2013;37:778-90.
13. Sung K, Daniel BL, Hargreaves BA. Transmit B1+ field inhomogeneity and T1 estimation errors in breast DCE-MRI at 3 tesla. J Magn Reson Imaging 2013;38:454-9.
14. Azlan CA, Di Giovanni P, Ahearn TS, Semple SI, Gilbert FJ, Redpath TW. B1 transmission-field inhomogeneity and enhancement ratio errors in dynamic contrast-enhanced MRI (DCE-MRI) of the breast at 3T. J Magn Reson Imaging 2010;31:234-9.
15. Kuhl CK, Kooijman H, Gieseke J, Schild HH. Effect of B1 inhomogeneity on breast MR imaging at 3.0 T. Radiology 2007;244:929-30.
16. Tsai WC, Kao KJ, Chang KM, Hung CF, Yang Q, Lin CE, *et al.* B(1) field correction of T1 estimation should be considered for breast dynamic contrast-enhanced MR imaging even at 1.5 T. Radiology 2017;282:55-62.
17. Bedair R, Graves MJ, Patterson AJ, McLean MA, Manavaki R, Wallace T, *et al.* Effect of radiofrequency transmit field correction on quantitative dynamic contrast-enhanced MR imaging of the breast at 3.0 T. Radiology 2016;279:368-77.
18. Pineda FD, Medved M, Fan X, Karczmar GS. B1 and T1 mapping of the breast with a reference tissue method. Magn Reson Med 2016;75:1565-73.
19. van Schie JJ, Lavini C, van Vliet LJ, Vos FM. Feasibility of a fast method for B1-inhomogeneity correction for FSPGR sequences. Magn Reson Imaging 2015;33:312-8.
20. Jena A, Mehta SB, Taneja S. Optimizing MRI scan time in the computation of pharmacokinetic parameters (K (trans)) in breast cancer diagnosis. J Magn Reson Imaging 2013;38:573-9.
21. Jena A, Taneja S, Singh A, Negi P, Mehta SB, Ahuja A, *et al.* Association of pharmacokinetic and metabolic parameters derived using simultaneous PET/MRI: Initial findings and impact on response evaluation in breast cancer. Eur J Radiol 2017;92:30-6.
22. Yuan J, Chow SK, Yeung DK, Ahuja AT, King AD. Quantitative evaluation of dual-flip-angle T1 mapping on DCE-MRI kinetic parameter estimation in head and neck. Quant Imaging Med Surg 2012;2:245-53.
23. Tofts PS, Brix G, Buckley DL, Evelhoch JL, Henderson E, Knopp MV, *et al.* Estimating kinetic parameters from dynamic contrast-enhanced T(1)-weighted MRI of a diffusable tracer: Standardized quantities and symbols. J Magn Reson Imaging 1999;10:223-32.
24. Deoni SC. High-resolution T1 mapping of the brain at 3T with driven equilibrium single pulse observation of T1 with high-speed incorporation of RF field inhomogeneities (DESPOT1-HIFI). J Magn Reson Imaging 2007;26:1106-11.
25. Veltman J, Stoutjesdijk M, Mann R, Huisman HJ, Barentsz JO, Blickman JG, *et al.* Contrast-enhanced magnetic resonance imaging of the breast: The value of pharmacokinetic parameters derived from fast dynamic imaging during initial enhancement in classifying lesions. Eur Radiol 2008;18:1123-33.
26. Brookes JA, Redpath TW, Gilbert FJ, Murray AD, Staff RT. Accuracy of T1 measurement in dynamic contrast-enhanced breast MRI using two-and three-dimensional variable flip angle fast low-angle shot. J Magn Reson Imaging 1999;9:163-71.
27. Zhang J, Winters K, Reynaud O, Kim SG. Simultaneous measurement of T(1)/B(1) and pharmacokinetic model parameters using active contrast encoding (ACE)-MRI. NMR Biomed 2017;30:10-1002.
28. Negi PS, Mehta SB, Jena A. Use of multiple-tube phantom: A method to globally correct native T1 relaxation time inhomogeneity in dedicated molecular magnetic resonance breast coil. J Med Phys 2021;46:41-6.
29. El Khouli RH, Macura KJ, Kamel IR, Jacobs MA, Bluemke DA. 3-T dynamic contrast-enhanced MRI of the breast: Pharmacokinetic parameters versus conventional kinetic curve analysis. AJR Am J Roentgenol 2011;197:1498-505.
30. Di Giovanni P, Azlan CA, Ahearn TS, Semple SI, Gilbert FJ, Redpath TW. The accuracy of pharmacokinetic parameter measurement in DCE-MRI of the breast at 3 T. Phys Med Biol 2010;55:121-32.

Time Intensity Curve Fitting and Smoothening

In the present scheme, VIBE sequence was used to acquire data in a discrete fashion (after every 4 s). Contrast concentration was calculated using these time-intensity points acquired up to 56 s (fourteen data point). These discrete points were fitted into best-fitted curve and smoothened to get a continuous curve to compute contrast concentration. In the proposed method, we used "least square approximation" method with "spline functions" to fit all the temporal points along the time-intensity curve [Supplementary Figure 1].[1]

Estimating the starting point of this curve was also important in computing contrast concentration called "time to start" [Supplementary Figure 2]. We analyzed the time intensity behavior of all cases and found that the rise of curve did not start before 5 s in "Plasma" and not before ten second in "Tissue." This was marked as point A. These points were used in calculating pharmacokinetic parameters. Fixing the starting point "A" was acceptable for most of the cases. But, hemodynamic variations in the patient depending on disease condition may cause variation in the starting point. An automatic method based on the intensity behavior of the neighboring time point along the rising curve was proposed, to find this point. Here, the intensity value of three subsequent time points (P1, P2, P3) along the curve was considered to find "time to start." The intensity value at each point was compared with the previous point, if the intensity value at P2 increases more than 10% from the previous point P1 and also intensity value at P3 >P2, then point P1 was regarded as the starting point of the curve. Auto selection of contrast arrival point (marking the starting point of the time-intensity graph) in our computation scheme was presumed to limit subjectivity in the user-defined fixed starting point and takes care of physiological variation in individual patient.

Step 1

Calculate T_{10} relaxation time of the tissue (before contrast) Equations 1, 2

For the evaluation of T_{10}, the non-fat suppressed T1 weighted pre-contrast 2° and 15° flip angle VIBE series were separately evaluated in phantom and patients. The Native T_1 was calculated with the help Equations 1, 2[2,3]

Equation 1 $$T_{10}^{-1} = \frac{1}{TR} \ln \left[\frac{S_R Sin\alpha 2 Cos\alpha 1 - Sin\alpha 1 Cos\alpha 2}{S_R Sin\alpha 2 - Sin\alpha 1} \right]$$

Equation 2 $$S_R = \frac{S_{\propto 1}}{S_{\propto 2}}$$

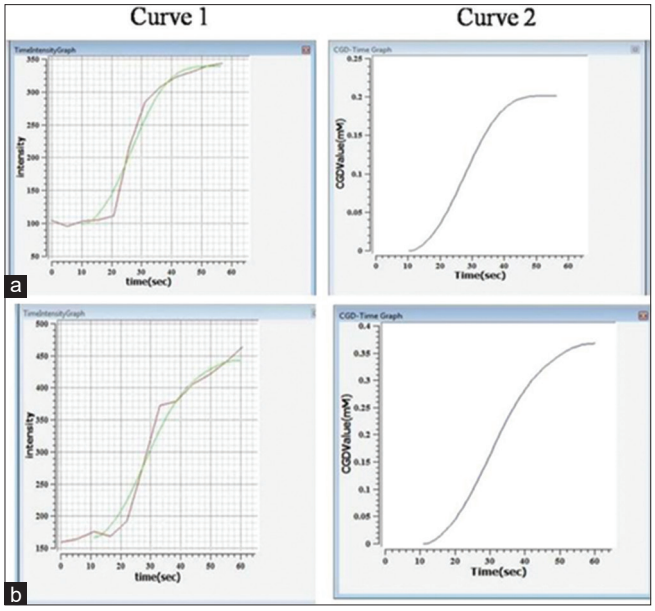

Supplementary Figure 1: (a) (Curve 1) Representative time-intensity curve and (Curve 2) Contrast concentration-Time curve for benign tissue (b) (Curve 1) Representative time-intensity curve and (Curve 2) Contrast concentration-Time curve for malignant tissue; red line in curve 1 and 2 is based on the spatial point and green line indicates curve-fitted and smoothed for different spatial points

Supplementary Table 1: T_{10} values of 51 enhancing breast lesions before and after correction

Noncorrected T_{10} ms		Corrected T_{10} ms	
Right	Left	Right	Left
1503.02	2122.97	1557.5	1804.67
1415.65	1948.92	1889.01	1475.89
1625.26	2133.84	1588.87	1966
1473.4	2468.01	1441.95	1847.99
1492.99	1666.33	1075.61	1530.4
1256.86	1882.13	1241.31	1428.78
1375.76	1690.4	1069.73	1309.67
922.317	1677.05	766.901	1643.26
1426.42	1503.02	1377.89	1657.38
1623.53	1434.82	1534.8	1361
1255.33	2112.77	1188.08	1885.4
1451.79	1309.67	1725.78	1121.29
1286.13	1883.13	1356.43	1786.5
1677.16	1588.71	2033.18	1315.22
1387.29	1875.73	1442.79	1541.5
1246.61	1966.45	1302.07	1794.75
1134.31	862.202	1245.21	724.119
1194.92	3301.66	1652.98	2983.5
1797.94	1612.22	2282.68	1661.6
1700.93	1774.16	1796.35	1864.37
1197.58	973.974	1239.22	940.333
2190.21	2974.88	2641.03	3172.81
2286.88	1836.38	2785.56	2150.44
1510.41	1692.21	1921.3	1295.66
1079.67	1522.25	1243.76	3172.81
1695.65		1941.66	
Mean=1469.54	Mean=1832.55	Mean=1590.06	Mean=1737.41
P=0.00411		*P*=0.34072	

$S\alpha_1$ = intensity value at $\alpha 1$ (2° flip angle), $S\alpha_2$ = intensity value at $\alpha 2$ (15° flip angle), TR = TR, In = Natural Log.

Reference native T_1 in phantom study

At the initial phase of our study, we imaged a vendor-provided phantom with known T_{10} value (280 ± 10 ms). When we imaged this phantom we found, the center of coil cuff to be the most homogenous part with T_{10} value 282.12 ± 11.32 for the right side and 285.66 ± 12.66 for the left.

The correction factors derived from this phantom when applied to breast lesions did not result in desired intensity ratio variation (ratio of 2° and 15° for the estimation of T_{10}) in breast tissue. To bifurcate this situation, we thought to change the phantom solution. In our experiment, we used gadolinium solution in the phantom as it is a commonly used MRI contrast agent and other researchers (Pineda *et al*. 2016) had also used this type of solution in their breast experiment.[4] The correction factors so derived from this new phantom solution had been used to normalize the T_{10} of coil cuff space.

As a first step, the mean T_1 value of the centrally placed tube (mean of 36 data points of central tube corresponding to 36 slices) of each coil cuffs were measured as 6.29 ± 0.22 ms; which was taken as a reference to find a deviation factor for each spatial location. Variations in T_1 value were documented for each breast coil from lateromedial, anteroposterior, and craniocaudal directions on each side, to calculate the correction factor at each spatial location. After applying the necessary correction factor, the T_1 value was calculated at each spatial location. The before and after correction T_1 were compared to assess the normalization.

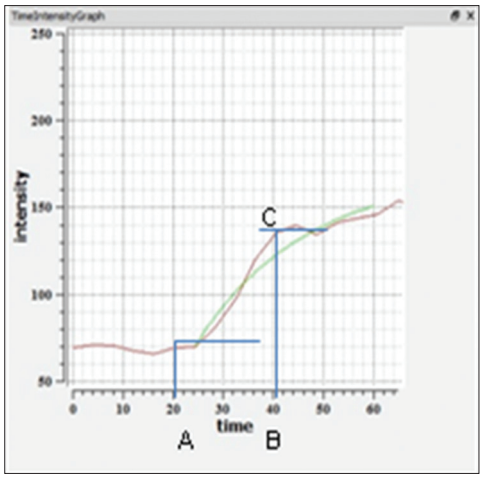

Supplementary Figure 2: Time-intensity curve of a malignant lesion computing native relaxation time T_{10}

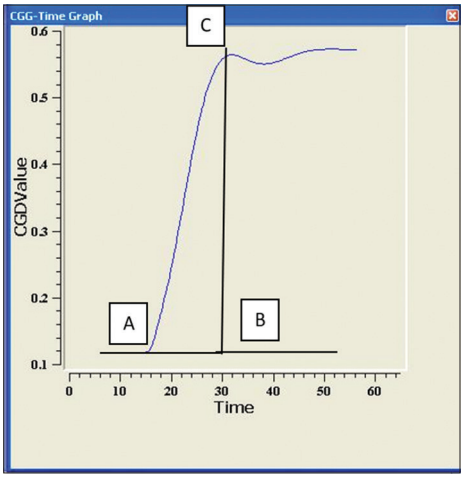

Supplementary Figure 3: Curve for contrast concentration of tissue with time ($C_{gdtissue}$)

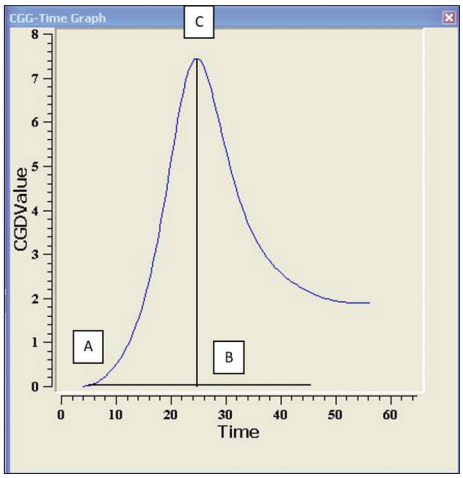

Supplementary Figure 4: Time-intensity curve for plasma. In the present study, a model AIF was taken that was derived from patient's data sets (mean plasma concentration with ROI over Aorta (large vessel)

Step 2

Correction Factor

Phantom T_1 was normalized with the help of correction factors derived for each spatial location by using Equations 3 and 4, and in turn, these correction factors were applied on patient's study to the corresponding spatial location for the calculation of corrected T_{10} and K^{trans}.[5]

Equation 3 $$Cf_n = \frac{Pht1 - t1_n}{Pht1}$$

$t1_n$ = Measured T_1 Value of phantom, Pht1 = T_1 value (6.29 ± 0.22 msec) of reference phantom, Cf_n = Correction Factor at each spatial location, n = Multi-tube phantom (1, 2,….19)

The formula used for correcting the T_{10} value

Equation 4 $$Ct1_n = UCt1_n + \left(UCt1_n * Cf_n\right)$$

$Ct1_n$ = Corrected T_{10}, Cf_n = Correction Factor, $UCt1_n$ = uncorrected T_{10}

For evaluation of the pharmacokinetic parameters from DCE images, nonfat-suppressed pre-contrast T1w VIBE series acquired at a 2° and 15° flip angles were used to calculate native T_1. Dynamic pre- and post-contrast VIBE series acquired at a 15° flip angle were used to calculate pharmacokinetic parameters K^{trans}, K_{ep}, v_e.

Step 3: Calculate T1 relaxation time at each time point

MRI Signal S of a tissue can be calculated as per the Bloch Equation 3

Equation 5 $$S = g.p.e^{-\frac{TE}{T2^*}} \frac{\sin \propto (1 - e^{-\frac{TR}{T1}})}{(1 - \cos \propto e^{-\frac{TR}{T1}})}$$

g is the gain factor and ρ is the proton density; $g.p.e^{-\frac{TE}{T2^*}}$ is S_0, a constant if T2* effect is neglected, and S1 and S (the pre contrast intrinsic tissue intensity) in Equations 3 and 4 considered as equivalent, the formula can be written as

Equation 6 $$S_0 = S_1 * \frac{1 - \cos \propto e^{-\frac{TR}{T_{10}}}}{\sin \propto (1 - e^{-\frac{TR}{T_{10}}})}$$

Now T_1 relaxation time at each temporal time point is calculated as per the Equation 4

Equation 7 $$\frac{1}{T_1(t)} = -\frac{1}{TR} In \frac{\sin \propto - S(t)/S_0}{\sin \propto - \cos \propto * S(t)/S_0}$$

Where S(t) is intensity value at each temporal point along the time intensity curve

$T_1(t)$ depicts the relaxation time at each temporal point

α is flip angle (15 degree) in the image sequence VIBE.

Step 4: Contrast estimation (Equation 8) at each voxel is based on T1 relaxation time at each temporal point as per Equation 7 above

Equation 8 $$C_{gdtissue}(t) = \frac{1}{r_1}\left[\frac{1}{T_1(t)} - \frac{1}{T_{10}}\right]$$

r1: relaxivity of the contrast agent

T_{10} is the native T_1 relaxation value of tissue before contrast.

$T_1(t)$ relaxation value at each temporal time point during DCE after contrast administration

In the present project we used Gadodiamide (Omniscan) with relaxivity value of 3.8 at 3 T. Supplementary Figure 3 shows the graphical representation of contrast concentration $C_{gdtissue}$ with time. Time point A is the time to start (when contrast arrived at tissue), time point B represents when contrast reaches peak value in the tissue, and point C is the peak contrast value.

Step 5: Measuring arterial input function

Contrast concentration $C_{gdplasma}$ C is calculated for each individual patient using time-intensity curve, similar to discussed as above in Equation 5, 6, 7. Here the time-intensity curve is drawn from the temporal images of an artery like aorta [Supplementary Figure 4]. Timepoint A is the time to start (when contrast arrived at plasma), time point B represents when contrast reaches peak value in the plasma, and point C is the peak contrast value. Here AIF is calculated for a tissue within the breast region as per the Equation 5, 6, 7.

The normalized T_{10} of tissue before and after Gd contrast administration was used to calculate Gd concentration in tissue ($C_{gdtissue}$) and plasma ($C_{gdplasma}$). For K^{trans} calculation arterial input function, TTP_{plasma} and TTP tissue were calculated with the help of in-house developed software

Calculation of pharmacokinetic parameters such as K^{trans}, k_{ep}, and v_e was done manually using the following equations.[6]

Equation 9 $$v_e = C_{gdtissue} / C_{gdplasma}$$

Equation 10 $$k_{ep} = \frac{1}{TTP_{tissue} - TTP_{plasma}}$$

Equation 11 $$K^{trans} = v_e * k_{ep}$$

Where $C_{gdtissue}$ is the concentration of contrast in the tissue, $C_{gdplasma}$ is the concentration of contrast in the plasma, TTP_{tissue} is the time to reach the peak intensity value in the tissue, and TTP_{plasma} is the time to reach the peak intensity in the plasma on the time intensity graph.

Supplementary References

1. Huisman HJ, Engelbrecht MR, Barentsz JO. Accurate estimation of pharmacokinetic contrast-enhanced dynamic MRI parameters of the prostate. J Magn Reson Imaging 2001;13:607-14.
2. Deichmann R, Haase A. Quantification of T1 values by SNAPSHOT-FLASH NMR imaging. J Mag Reson Imaging 1992;96:608-12.
3. Rakow-Penner R, Daniel B, Yu H, Sawyer-Glover A, Glover GH. Relaxation times of breast tissue at 1.5T and 3T measured using IDEAL. J Magn Reson Imaging 2006;23:87-91.
4. Pineda FD, Medved M, Fan X, Karczmar GS. B1 and T1 mapping of the breast with a reference tissue method. Magn Reson Med 2016;75:1565-73.
5. Negi PS, Mehta SB, Jena A. Use of multiple-tube phantom: A method to globally correct native T1 relaxation time inhomogeneity in dedicated molecular magnetic resonance breast coil. J Med Phys 2021;46:41-6.
6. Veltman J, Stoutjesdijk M, Mann R, Huisman HJ, Barentsz JO, Blickman JG, *et al.* Contrast-enhanced magnetic resonance imaging of the breast: The value of pharmacokinetic parameters derived from fast dynamic imaging during initial enhancement in classifying lesions. Eur Radiol 2008;18:1123-33.